

PAPER

Near-field imaging of scattering obstacles with the factorization method

To cite this article: Guanghui Hu *et al* 2014 *Inverse Problems* **30** 095005

View the [article online](#) for updates and enhancements.

Related content

- [Near-field imaging of obstacles with the factorization method: fluid–solid interaction](#)
Tao Yin, Guanghui Hu, Liwei Xu *et al*.
- [An approximate factorization method for inverse medium scattering with unknown buried objects](#)
Fenglong Qu, Jiaqing Yang and Bo Zhang
- [Some inverse problems arising from elastic scattering by rigid obstacles](#)
Guanghui Hu, Andreas Kirsch and Mourad Sini

Recent citations

- [Near field imaging of small isotropic and extended anisotropic scatterers](#)
I. Harris and S. Rome
- [Factorization method in inverse interaction problems with bi-periodic interfaces between acoustic and elastic waves](#)
Guanghui Hu *et al*
- [Near-field imaging of obstacles with the factorization method: fluid–solid interaction](#)
Tao Yin *et al*

Near-field imaging of scattering obstacles with the factorization method

Guanghui Hu¹, Jiaqing Yang², Bo Zhang³ and Haiwen Zhang⁴

¹Weierstrass Institute for Applied Analysis and Stochastics, Mohrenstr 39, D-10117 Berlin, Germany

²Academy of Mathematics and Systems Science, Chinese Academy of Sciences, Beijing 100190, People's Republic of China

³LSEC and Institute of Applied Mathematics, AMSS, Chinese Academy of Sciences, Beijing 100190, People's Republic of China

⁴Institute of Automation, Chinese Academy of Sciences, Beijing 100190, People's Republic of China

E-mail: hu@wias-berlin.de, jiaqingyang@amss.ac.cn, b.zhang@amt.ac.cn and zhanghaiwen@amss.ac.cn

Received 25 May 2014, revised 14 July 2014

Accepted for publication 17 July 2014

Published 20 August 2014

Abstract

In this paper we establish a factorization method for recovering the location and shape of an acoustic bounded obstacle with using the near-field data, corresponding to infinitely many incident point sources. The obstacle is allowed to be an impenetrable scatterer of sound-soft, sound-hard or impedance type or a penetrable scatterer. An outgoing-to-incoming operator is constructed for facilitating the factorization of the near-field operator, which can be easily implemented numerically. Numerical examples are presented to demonstrate the feasibility and effectiveness of our inversion algorithm, including the case where limited aperture near-field data are available only.

Keywords: factorization method, inverse scattering, near-field data, Helmholtz equation, point sources

(Some figures may appear in colour only in the online journal)

1. Introduction

This paper is concerned with the inverse problem of scattering of time-harmonic acoustic waves from a bounded obstacle at a fixed frequency. Denoted by D the bounded obstacle in \mathbb{R}^3 with the boundary $\partial D \in \mathcal{C}^2$. Then the scattering problem is modeled by

$$\begin{cases} \Delta u + k^2 u = 0 & \text{in } \mathbb{R}^3 \setminus \bar{D}, \\ \mathcal{B}u = f & \text{on } \partial D, \\ \lim_{r \rightarrow \infty} r \left(\frac{\partial u}{\partial r} - iku \right) = 0 & \text{with } r = |x|, \end{cases} \quad (1.1)$$

where $k > 0$ is the wave number and \mathcal{B} denotes the boundary condition imposed on ∂D . For a sound-soft obstacle, the scattered field u satisfies the Dirichlet boundary condition

$$\mathcal{B}u := u = f \quad \text{on } \partial D, \quad (1.2)$$

whereas for an imperfect or partially coated obstacle, u satisfies the impedance boundary condition

$$\mathcal{B}u := \frac{\partial u}{\partial \nu} + \rho(x)u = f \quad \text{on } \partial D. \quad (1.3)$$

In (1.3), the normal ν to the boundary ∂D is assumed to be outward and $\rho(x) \in L^\infty(\partial D)$ is the given (complex-valued) impedance function with $\text{Im}(\rho) \geq 0$. In the case $\rho(x) \equiv 0$ on ∂D , the impedance boundary condition (1.3) reduces to the classical Neumann boundary condition

$$\mathcal{B}u := \frac{\partial u}{\partial \nu} = f \quad \text{on } \partial D.$$

In this paper, we consider the point source wave as the incident wave $u^i(x, y)$ which is generated at the source position $y \in \mathbb{R}^3$:

$$u^i(x, y) = \Phi(x, y) = \frac{e^{ik|x-y|}}{4\pi|x-y|}, \quad y \in \mathbb{R}^3 \setminus \bar{D}, \quad x \neq y,$$

and the corresponding scattered field is denoted by $u(x, y)$ which depends on the point source position y . It is well-known that $\Phi(x, y)$ is the free-space fundamental solution to the Helmholtz equation $(\Delta + k^2)v = 0$ in \mathbb{R}^3 . Then the boundary data f in (1.1) is given as $f := -\mathcal{B}u^i(\cdot, y)$.

The last condition in (1.1) is known as the Sommerfeld radiation condition, allowing the scattered field $u(x, y)$ to have the asymptotic behavior

$$u(x, y) = \frac{e^{ik|x|}}{4\pi|x|} \left\{ u^\infty(\hat{x}, y) + O\left(\frac{1}{|x|}\right) \right\} \quad \text{as } |x| \rightarrow \infty$$

uniformly in all directions $\hat{x} = x/|x|$. The function $\hat{x} \rightarrow u^\infty(\hat{x}, y)$ is called the far-field pattern of $u(x, y)$, which is an analytic function defined on the unit sphere $\mathbb{S}^2 := \{x: |x| = 1\}$. Here, we have emphasized the dependence of $u^\infty(\hat{x}, y)$ on the point source position y . Since the function $\Phi(x, \cdot)$ is also a radiating solution, it behaves like

$$\Phi(x, y) = \frac{e^{ik|y|}}{4\pi|y|} \left\{ e^{ikx \cdot d} + O\left(\frac{1}{|y|}\right) \right\} \quad \text{as } |y| \rightarrow \infty, \quad d := -\hat{y} \in \mathbb{S}^2. \quad (1.4)$$

Hence, as a function of $x \in \mathbb{R}^3$, the far-field pattern $e^{ikx \cdot d}$ of the point source $\Phi(x, y)$ is exactly the plane wave propagating at the direction $d = -\hat{y}$.

Set $B_R := \{x: |x| < R\}$, $S_R := \{x: |x| = R\}$ and assume that there is *a priori* information that $D \subset B_R$ for some large $R > 0$. Our concern in this paper is to recover ∂D from the near-field data $\{u(x, y): x, y \in S_R\}$ by sending incident point sources $u^i(x, y)$ with $y \in S_R$. It is well-known that D can be uniquely determined from the far-field pattern $u^\infty(\hat{x}; d)$ of all incident plane waves $u^i(x) = e^{ikx \cdot d}$ with $\hat{x}, d \in \mathbb{S}^2$ (see, e.g. [6]). Such a uniqueness result could be easily extended to the case with near-field data by using Rellich's lemma and the mixed

reciprocity relation (see, e.g. [2]). Hence, the obstacle D is uniquely determined by the scattered near-field $u(\cdot; y)|_{S_R}$ for all $y \in S_R$. In this paper, we will also present a short proof based on the symmetric relation of the fundamental solution to the scattering problem by utilizing limited aperture near-field data only (see theorem 3.9).

The factorization method in inverse scattering was first introduced by Kirsch [4] in 1998 and has been extended and improved continuously since then; see the monograph [7] and the survey paper [3]. It provides a necessary and sufficient criterion for precisely characterizing the shape and location of the scattering obstacle, utilizing the spectral system of the so-called far-field operator defined by the far-field pattern. Recently we have generalized the factorization method to the case of penetrable obstacles with unknown buried objects [11] and the case of complex impenetrable obstacles with generalized impedance boundary conditions [12].

In the case of incident plane waves, to apply the factorization method one needs to investigate the far-field operator $F: L^2(\mathbb{S}^2) \rightarrow L^2(\mathbb{S}^2)$ defined by

$$(Fg)(\hat{x}) = \int_{\mathbb{S}^2} u^\infty(\hat{x}; d)g(d)ds(d) \quad \text{for } \hat{x} \in \mathbb{S}^2. \quad (1.5)$$

In a framework of functional analysis, the above operator F can be factorized into the form LTL^* , where the adjoint operator L^* is defined via a sesquilinear form in the sense of the extension of L^2 -inner product. Then a connection between the operators F and L is established by a range identity (see, e.g. [7]) and the characteristic function of the scatterer can be constructed in term of the spectral system of the far-field operator.

In many applications, the measurement data are taken not very far away from the scatterer (compared to the wavelength), and point source waves are usually used as incident fields. We then need to consider the near-field operator $N: L^2(S_R) \rightarrow L^2(S_R)$ defined by

$$(Ng)(x) = \int_{S_R} u(x, y)g(y)ds(y) \quad \text{for } x \in S_R. \quad (1.6)$$

However, as far as we know, it is still an open problem how to develop a factorization method with near-field data which is efficient in computation, through establishing an appropriate factorization of N directly (as for the far-field operator F). The functional framework for factorizing the far-field operator F does not extend to the near-field operator N since the resulting adjoint for N would be defined via a bilinear other than sesquilinear form giving arise to essential difficulties in the characterization of D (see [7, chapter 1.7] for details). To overcome such a difficulty, three main approaches have been proposed so far. One is to convert the near-field operator N into the far-field operator F , based on the mixed reciprocity relation, so our inverse problem can then be reduced to the visualization problem from the far-field operator $F = P_1NP_2$ with certain auxiliary operators P_1 and P_2 ; see [7] and [10] for details. It should be remarked that this approach cannot apply to the case where limited aperture near-field data are available since the full data on S_R is needed in order to compute the far-field pattern. Further, this approach seems not efficient in computation. Another approach was also proposed in [10]. The idea is to connect outgoing and incoming waves by constructing non-physical auxiliary operators which seem difficult to implement numerically. The third approach is to use non-physical incident point sources (i.e., $\overline{\Phi(x; y)}$) to generate a non-physical near-field operator N_{np} . One can first develop a factorization method for N_{np} and then prove that the non-physical near-field operator can be approximated by regularized physical ones in the sense that $NP_\delta \rightarrow N_{np}$ in some sense as $\delta \rightarrow 0$ for certain operator P_δ . Thus the non-physical near-field operator N_{np} can be regarded as a regularized physical one

NP_δ for a very small δ . This approach was first proposed in [8] and then improved in [1]; see [1, 8] for details.

In this paper we will develop a framework for establishing the factorization method for recovering ∂D from the near-field data, which is computationally efficient and easy to implement. Our approach is to construct an unitary operator T_1 on $L^2(S_R)$, which is an outgoing-to-incoming operator in the sense of remark 3.3 below and has a very simple form so that it can be easily implemented numerically. Then a factorization of $T_1 N$ can be derived in the standard way, so the range identity from [7] is still applicable. We will prove that our imaging scheme is independent of the boundary conditions on ∂D since it applies to sound-soft, sound-hard and impedance-type impenetrable obstacles as well as penetrable obstacles. Moreover, the case of limited aperture near-field data can be treated as well; see the discussion at the end of section 3.2. The developed factorization method with the near-field data is comparable with that using the far-field data. For simplicity we only consider the three-dimensional case and the case where the measurement is taken at the sphere S_R . However, our analysis extends easily to the two-dimensional case and the case where the measurement surface is taken as a star-shaped continuous surface M which encloses the obstacle D and is given by the form $|x| = \phi(\hat{x})$, that is, $M = \{x \in \mathbb{R}^3: x = \phi(\hat{x})\hat{x}\}$ (see remark 3.4 below for details).

The remaining part of the paper is organized as follows. In section 2, we derive the Fourier coefficients of the near-field operator with respect to the spherical harmonics. Section 3 is devoted to a justification of the factorization method for identifying sound-soft obstacles. The definition of the outgoing-to-incoming operator T_1 is given in section 3.1, and an explicit example for recovering the sound-soft unit ball is presented in section 3.3. In the subsequent sections 4 and 5, the factorization method is extended to the case of other boundary conditions such as the impedance and Neumann conditions and the inverse medium scattering case, respectively. In section 6, numerical examples are presented to illustrate the feasibility and effectiveness of the inversion algorithm.

2. Fourier coefficients of near-field operator

We begin with the normalized spherical harmonic functions of order n , given by

$$Y_n^m(\theta, \varphi) := \sqrt{\frac{2n+1}{4\pi} \frac{(n-|m|)!}{(n+|m|)!}} P_n^{|m|}(\cos \theta) e^{im\varphi}, \quad n = 0, 1, 2, \dots, \quad m = -n, \dots, n,$$

where (θ, φ) represents the spherical coordinates on the unit sphere \mathbb{S}^2 and P_n^m are the associated Legendre functions. By definition it holds that $Y_n^{-m} = \overline{Y_n^m}$. It is well-known that $\{Y_n^m: n \in \mathbb{N}, m = -n, \dots, n\}$ forms a complete orthonormal system in $L^2(\mathbb{S}^2)$. Thus, for each $g \in L^2(S_R)$ we have the expansion

$$g(x) = \sum_{n=0}^{\infty} \sum_{m=-n}^n g_{n,m} Y_n^m(\hat{x}) \quad \text{with} \quad g_{n,m} := \frac{1}{R^2} \int_{S_R} g(x) \overline{Y_n^m(\hat{x})} ds, \quad (2.1)$$

where the coefficients $g_{n,m} \in \mathbb{C}$ are referred to as the Fourier coefficients of g with respect to the spherical harmonics. Throughout the paper the Fourier coefficients of an L^2 function on S_R are understood in this sense. Observing that

$$\|g\|_{L^2(S_R)}^2 = R^2 \sum_{n=0}^{\infty} \sum_{m=-n}^n |g_{n,m}|^2,$$

we define the operator $\mathcal{F}_R: L^2(S_R) \rightarrow \ell^2$ by

$$\mathcal{F}_R(\mathbf{g}) = \mathbf{g}, \quad \mathbf{g} := \{g_{n,m}: n \in \mathbb{N}, m = -n, \dots, n\} \in \ell^2. \quad (2.2)$$

Conversely, for $\mathbf{g} = \{g_{n,m}: n \in \mathbb{N}, m = -n, \dots, n\} \in \ell^2$ we can define the operator $\mathcal{F}_R^{-1}: \ell^2 \rightarrow L^2(S_R)$ by

$$\mathcal{F}_R^{-1}(\mathbf{g}) = \sum_{n=0}^{\infty} \sum_{m=-n}^n g_{n,m} Y_n^m(\hat{x}) \quad \text{on } |x| = R. \quad (2.3)$$

Further, it can be readily deduced from (2.2) and (2.3) that

$$\mathcal{F}_R \mathcal{F}_R^{-1} = I_{\ell^2}, \quad \mathcal{F}_R^{-1} \mathcal{F}_R = I_{L^2(S_R)}, \quad \mathcal{F}_R^* = \frac{1}{R^2} \mathcal{F}_R^{-1}, \quad (\mathcal{F}_R^{-1})^* = R^2 \mathcal{F}_R, \quad (2.4)$$

where I_{ℓ^2} and $I_{L^2(S_R)}$ denote the identity operator on ℓ^2 and $L^2(S_R)$, respectively.

Let j_n and $h_n^{(1)}$ be the spherical Bessel functions and spherical Hankel functions of order n , respectively. Set

$$u_{n,m}^i(x) = j_n(k|x|) Y_n^m(\hat{x}), \quad x \in \mathbb{R}^3, \quad n \in \mathbb{N}, m = -n, \dots, n.$$

It is well known that $u_{n,m}^i$ are entire solutions to the Helmholtz equation $\Delta u + k^2 u = 0$ in \mathbb{R}^3 . Denote by $u_{n,m}$ the unique radiating solution to the problem (1.1) with $f := -(\mathcal{B}u_{n,m}^i)|_{\partial D}$, which can be regarded as the scattered field corresponding to the incident wave $u_{n,m}^i$. It is shown in [2, Theorem 215] that $u_{n,m}$ has the expansion

$$u_{n,m}(x) = \sum_{p=0}^{\infty} \sum_{q=-p}^p a_{p,q}^{n,m} h_p^{(1)}(k|x|) Y_p^q(\hat{x}), \quad a_{p,q}^{n,m} \in \mathbb{C}, \quad (2.5)$$

which converges absolutely and uniformly on compact subsets of $|x| > R$. Therefore,

$$\mathcal{F}_R \left(u_{n,m} \Big|_{S_R} \right) = \{ a_{p,q}^{n,m} h_p^{(1)}(kR): p \in \mathbb{N}, q = -p, \dots, p \} \in \ell^2$$

for all $n \in \mathbb{N}, m = -n, \dots, n$. Instead of the near-field operator N , we will consider the operator

$$\mathcal{N} := \mathcal{F}_R N \mathcal{F}_R^{-1}: \ell^2 \rightarrow \ell^2, \quad (2.6)$$

defined by using the Fourier coefficients of g and Ng on S_R . An explicit expression of \mathcal{N} is given as follows.

Lemma 2.1. *Let $g, g_{n,m}, \mathbf{g}$ and $a_{p,q}^{n,m}$ be given as in (2.1), (2.2) and (2.5), respectively. Then it holds that*

$$\mathcal{N} \mathbf{g} = \left\{ ikR^2 h_p^{(1)}(kR) \sum_{n=0}^{\infty} \sum_{m=-n}^n a_{p,q}^{n,m} h_n^{(1)}(kR) g_{n,m}: p \in \mathbb{N}, q = -p, \dots, p \right\}. \quad (2.7)$$

Proof. By definition, $\mathcal{N} \mathbf{g} = \mathcal{F}_R N g$. Thus we only need to derive the Fourier coefficients of the near-field data Ng with respect to the spherical harmonics. Set $U(x) := \int_{S_R} u(x, y) g(y) ds(y)$ for $x \in \mathbb{R}^3 \setminus \bar{D}$. Clearly, Ng is the restriction to S_R of U with

U being the scattered field corresponding to the incident field $U^i(x) := \int_{S_R} \Phi(x, y) g(y) ds(y)$ for $|x| < R$. Recall (see [2, Theorem 2.11]) that the fundamental solution Φ has the expansion

$$\Phi(x, y) = ik \sum_{n=0}^{\infty} \sum_{m=-n}^n h_n^{(1)}(k|y|) Y_n^m(\hat{y}) j_n(k|x|) \overline{Y_n^m(\hat{x})}, \quad (2.8)$$

which converges absolutely and uniformly on compact subsets of $|x| < |y|$. Since $Y_n^m = \overline{Y_n^{-m}}$, one can rewrite the previous identity as

$$\Phi(x, y) = ik \sum_{n=0}^{\infty} \sum_{m=-n}^n h_n^{(1)}(k|y|) \overline{Y_n^m(\hat{y})} j_n(k|x|) Y_n^m(\hat{x}) \quad \text{for } |x| < |y|.$$

This implies that for $|x| < R$,

$$\begin{aligned} U^i(x) &= ikR^2 \sum_{n=0}^{\infty} \sum_{m=-n}^n h_n^{(1)}(kR) g_{n,m} \left[j_n(k|x|) Y_n^m(\hat{x}) \right] \\ &= ikR^2 \sum_{n=0}^{\infty} \sum_{m=-n}^n h_n^{(1)}(kR) g_{n,m} u_{n,m}^i(x), \end{aligned} \quad (2.9)$$

with $g_{n,m}$ defined by (2.1). Then, by linear superposition we conclude from (2.5) and (2.9) that

$$\begin{aligned} U(x) &= ikR^2 \sum_{n=0}^{\infty} \sum_{m=-n}^n h_n^{(1)}(kR) g_{n,m} u_{n,m}(x) \\ &= ikR^2 \sum_{n=0}^{\infty} \sum_{m=-n}^n h_n^{(1)}(kR) g_{n,m} \left(\sum_{p=0}^{\infty} \sum_{q=-p}^p a_{p,q}^{n,m} h_p^{(1)}(k|x|) Y_p^q(\hat{x}) \right) \\ &= ikR^2 \sum_{p=0}^{\infty} \sum_{q=-p}^p h_p^{(1)}(k|x|) \left(\sum_{n=0}^{\infty} \sum_{m=-n}^n a_{p,q}^{n,m} h_n^{(1)}(kR) g_{n,m} \right) Y_p^q(\hat{x}), \end{aligned} \quad (2.10)$$

for $|x| > R$. Here, interchanging the order of summation is allowed since the two series converge absolutely and uniformly on compact subsets of $|x| > R$. The Fourier coefficients of $U(x)|_{S_R}$ in (2.10) finally yield the expression (2.7). \square

3. Dirichlet boundary condition

In this section, we will establish the factorization method for reconstructing a sound-soft obstacle from near-field data corresponding to incident point source waves. The key ingredients in our analysis consist of the construction of an outgoing-to-incoming mapping T_1 and an appropriate factorization of the operator $T_1 N$.

3.1. Factorization of near-field operator

Similarly to the Herglotz wave function for plane waves, we define the incidence operator $H_{Dir}: \ell^2 \rightarrow H^{1/2}(\partial D)$ for the Dirichlet boundary value problem by (see (2.9)):

$$H_{Dir}(\mathbf{g}) = U^i|_{\partial D} = ikR^2 \sum_{n=0}^{\infty} \sum_{m=-n}^n h_n^{(1)}(kR) g_{n,m} u_{n,m}^i(x), \quad x \in \partial D.$$

The operator H_{Dir} maps a superposition of the incident waves $u_{n,m}^i$ with the weight $g_{n,m}$ into its trace on ∂D . Since j_n is real-valued, the adjoint operator $H_{Dir}^*: H^{-1/2}(\partial D) \rightarrow \ell^2$ is given by

$$H_{Dir}^* \psi = \left\{ -ikR^2 \overline{h_n^{(1)}(kR)} \int_{\partial D} \psi(y) j_n(k|y|) \overline{Y_n^m(\hat{y})} ds(y) : n \in \mathbb{N}, m = -n, \dots, n \right\}. \quad (3.1)$$

Denote by u the unique outgoing radiating solution to the problem (1.1) with the boundary value $f \in H^{1/2}(\partial D)$. Suppose that on $|x| = R$,

$$u(x)|_{S_R} = \sum_{n=0}^{\infty} \sum_{m=-n}^n b_n^m h_n^{(1)}(kR) Y_n^m(\hat{x}), \quad b_n^m \in \mathbb{C}.$$

Then the Fourier coefficients of $u|_{S_R}$ define the solution operator $G_{Dir} : H^{1/2}(\partial D) \rightarrow \ell^2$ as

$$G_{Dir}(f) := \left\{ b_n^m h_n^{(1)}(kR) : n \in \mathbb{N}, m = -n, \dots, n \right\}. \quad (3.2)$$

From the definition of \mathcal{N} , G_{Dir} and H_{Dir} the following relation follows:

$$\mathcal{N} = -G_{Dir} H_{Dir}. \quad (3.3)$$

As for the incident plane wave case, we introduce the single-layer operator and single-layer potential

$$\begin{aligned} (S\psi)(x) &= \int_{\partial D} \Phi(x, y) \psi(y) ds(y), \quad x \in \partial D, \\ (V\psi)(x) &= \int_{\partial D} \Phi(x, y) \psi(y) ds(y), \quad x \in \mathbb{R}^3 \end{aligned}$$

for $\psi \in H^{-1/2}(\partial D)$. It follows from the expansion (2) that for $|x| \geq R$,

$$(V\psi)(x) = ik \sum_{n=0}^{\infty} \sum_{m=-n}^n h_n^{(1)}(k|x|) \left[\int_{\partial D} \psi(y) j_n(k|y|) \overline{Y_n^m(\hat{y})} ds \right] Y_n^m(\hat{x}).$$

This, together with the definition of G_{Dir} and the jump relations for single-layer potentials, implies that

$$\begin{aligned} G_{Dir}((V\psi)|_{\partial D}) &= G_{Dir} S\psi \\ &= \left\{ ik h_n^{(1)}(kR) \int_{\partial D} \psi(y) j_n(k|y|) \overline{Y_n^m(\hat{y})} ds : n \in \mathbb{N}, m = -n, \dots, n \right\}. \end{aligned} \quad (3.4)$$

Remark 3.1. Comparing (3.1) and (3.4), it is observed that the relation $G_{Dir} S = H_{Dir}^*$, which is true for the far-field operator, does not hold in the present case. It is the reason why the operator \mathcal{N} (also the near-field operator N) cannot be factorized in a straightforward way.

To find out an appropriate factorization of \mathcal{N} , we observe further from (3.1) and (3.4) that

$$R^2 T_0 G_{Dir} S = H_{Dir}^* \quad \text{or equivalently} \quad R^2 S^* G_{Dir}^* T_0^* = H_{Dir}, \quad (3.5)$$

where the operator $T_0: \ell^2 \rightarrow \ell^2$ is defined as

$$T_0(\mathbf{g}) = \left\{ -\frac{\overline{h_n^{(1)}(kR)}}{h_n^{(1)}(kR)} g_{n,m} : n \in \mathbb{N}, m = -n, \dots, n \right\}, \quad (3.6)$$

for $\mathbf{g} = \{g_{n,m} : n \in \mathbb{N}, m = -n, \dots, n\} \in \ell^2$. Note that T_0 is well-defined in ℓ^2 since $h_n^{(1)}(kR) \neq 0$ for all $n \in \mathbb{N}$. Moreover, it is seen from (3.6) that T_0 is a unitary operator on ℓ^2 , that is, $T_0 T_0^* = T_0^* T_0 = I_{\ell^2}$. From (3.3) and the second relation in (3.5) it follows that

$$T_0 \mathcal{N} = -T_0 G_{Dir} H_{Dir} = -R^2 (T_0 G_{Dir}) S^* (T_0 G_{Dir})^*. \quad (3.7)$$

Accordingly, a factorization of the near-field operator can be obtained as follows.

Theorem 3.2. *We have the factorization*

$$T_1 N = -\mathbb{G}_{Dir} S^* \mathbb{C}_{Dir}^*, \quad \mathbb{G}_{Dir} := \mathcal{F}_R^{-1} T_0 G_{Dir}, \quad (3.8)$$

where $T_1 := \mathcal{F}_R^{-1} T_0 \mathcal{F}_R: L^2(S_R) \rightarrow L^2(S_R)$ takes the form

$$(T_1 g)(x) = \int_{S_R} K(x, y) g(y) ds(y) \quad \text{for } g \in L^2(S_R), \quad (3.9)$$

with the kernel

$$K(x, y) := -\frac{1}{4\pi R^2} \sum_{n=0}^{\infty} \left(\frac{\overline{h_n^{(1)}(kR)}}{h_n^{(1)}(kR)} \right) (2n+1) P_n(\cos \theta). \quad (3.10)$$

In (3.10), P_n are the Legendre polynomials and θ denotes the angle between $x \in S_R$ and $y \in S_R$.

Proof. From the definition of \mathcal{F}_R , N and \mathcal{N} it follows that $N = \mathcal{F}_R^{-1} \mathcal{N} \mathcal{F}_R$. In view of the factorization of $T_0 \mathcal{N}$ (see (3.7)) and the definition of T_1 , it is derived that

$$\begin{aligned} T_1 N &= \mathcal{F}_R^{-1} (T_0 \mathcal{N}) \mathcal{F}_R = -R^2 \mathcal{F}_R^{-1} (T_0 G_{Dir}) S^* (T_0 G_{Dir})^* \mathcal{F}_R \\ &= -(\mathcal{F}_R^{-1} T_0 G_{Dir}) S^* (\mathcal{F}_R^{-1} T_0 G_{Dir})^*, \end{aligned} \quad (3.11)$$

where the last equality follows from the last relation in (2.4). This gives the factorization (3.8) with the operator \mathbb{G}_{Dir} given as above.

By the definition of T_1 and T_0 it follows that for $g \in L^2(S_R)$,

$$(T_1 g)(x) = -\sum_{n=0}^{\infty} \sum_{m=-n}^n \left(\frac{\overline{h_n^{(1)}(kR)}}{h_n^{(1)}(kR)} g_{n,m} \right) Y_n^m(\hat{x}), \quad x \in S_R \quad (3.12)$$

with $g_{n,m} := R^{-2} \int_{S_R} g(x) \overline{Y_n^m(\hat{x})} ds(x)$. Making use of the *addition theorem* (see, e.g., [2, Theorem 2.8]), we can reformulate the previous identity as

$$\begin{aligned} (T_1 g)(x) &= -\sum_{n=0}^{\infty} \sum_{m=-n}^n \left(\frac{\overline{h_n^{(1)}(kR)}}{h_n^{(1)}(kR)} \right) Y_n^m(\hat{x}) \left(\frac{1}{R^2} \int_{S_R} g(y) \overline{Y_n^m(\hat{y})} ds(y) \right) \\ &= -\frac{1}{R^2} \int_{S_R} g(y) \sum_{n=0}^{\infty} \left(\frac{\overline{h_n^{(1)}(kR)}}{h_n^{(1)}(kR)} \right) \left(\sum_{m=-n}^n Y_n^m(\hat{x}) \overline{Y_n^m(\hat{y})} \right) ds(y) \\ &= \int_{S_R} K(x, y) g(y) ds(y) \end{aligned}$$

with the kernel $K(x, y)$ given by (3.10). The proof is thus complete. \square

Remark 3.3. The operator T_1 is essentially an outgoing-to-incoming mapping in the following sense. Let v be an outgoing solution to the Helmholtz equation which satisfies the outgoing Sommerfeld radiation condition. Suppose v admits the expansion

$$v(x) = \sum_{n=0}^{\infty} \sum_{m=-n}^n v_{n,m} h_n^{(1)}(k|x|) Y_n^m(\hat{x}) \quad \text{for all } |x| > R_0 > 0.$$

Define the incoming wave

$$\tilde{v}(x) = - \sum_{n=0}^{\infty} \sum_{m=-n}^n v_{n,m} \overline{h_n^{(1)}(k|x|)} Y_n^m(\hat{x}) \quad \text{for all } |x| > R_0.$$

Then the function \tilde{v} satisfies the Helmholtz equation and the incoming condition

$$\lim_{r \rightarrow \infty} r \left(\frac{\partial \tilde{v}}{\partial r} + ik\tilde{v} \right) = 0, \quad r = |x|.$$

Then, by (3.12) it can be readily verified that

$$T_1 \left(v \Big|_{S_R} \right) = \tilde{v} \Big|_{S_R} \quad \text{for all } R > R_0.$$

In particular, we have (see (3.16) in section 3.2 below)

$$T_1 \left(\Phi(\cdot, z) \Big|_{S_R} \right) = \overline{\Phi(\cdot, z)} \Big|_{S_R} \quad \text{for all } R > |z|.$$

Remark 3.4. As mentioned in the introduction, our method also works for the case where the measurement is taken at a star-shaped continuous surface M enclosing the obstacle D and taking the form $|x| = \phi(\hat{x})$, that is, $M = \{x \in \mathbb{R}^3: x = \phi(\hat{x})\hat{x}\}$ with ϕ a positive and continuous function on the unit sphere \mathbb{S}^2 . However, in this case, the operator $T_1: L^2(M) \rightarrow L^2(M)$ has a complicated expression, so $T_1 N$ is not so easy to discretize.

3.2. Inversion algorithm and a uniqueness result

We first show the properties of the solution operator G_{Dir} defined by (3.2) and the modified solution operator \mathbb{G}_{Dir} (see (3.8)).

Lemma 3.5.

- (i) The solution operator $G_{Dir}: H^{1/2}(\partial D) \rightarrow \ell^2$ is compact, one-to-one with a dense range in ℓ^2 .
- (ii) The operator $\mathbb{G}_{Dir}: H^{1/2}(\partial D) \rightarrow L^2(S_R)$ is compact, one-to-one with a dense range in $L^2(S_R)$.

Proof. (i) The injectivity of G_{Dir} simply follows from the uniqueness of the exterior Dirichlet problem and the analytic continuation argument. The compactness is a consequence of the well-posedness of the scattering problem (1.1) in $H_{loc}^1(\mathbb{R}^3 \setminus \overline{D})$ and the compact embedding property of $H^{1/2}(S_R)$ into $L^2(S_R)$.

To prove that the range of G_{Dir} is dense in ℓ^2 , define the sequence $\mathbf{g}^{(M)} \in \ell^2$ with some $M \in \mathbb{N}$ by

$$\mathbf{g}^{(M)} = \left\{ \mathbf{g}_{n,m}^{(M)} : n \in \mathbb{N}, m = -n, \dots, n \right\}, \quad \mathbf{g}_{n,m}^{(M)} := \begin{cases} g_{n,m}, & n \leq M \\ 0, & n > M \end{cases}$$

for every $\mathbf{g} = \{g_{n,m}: n \in \mathbb{N}, m = -n, \dots, n\} \in \ell^2$. Then, for any $\epsilon > 0$ there exists a $M_\epsilon > 0$ such that $\|\mathbf{g}^{(M_\epsilon)} - \mathbf{g}\|_{\ell^2} < \epsilon$. Choose the origin inside of D and define the

function v by

$$v(x) = \sum_{n=0}^{M_\epsilon} \sum_{m=-n}^n \left(\frac{1}{h_n^{(1)}(kR)} g_{n,m} \right) h_n^{(1)}(k|x|) Y_n^m(\hat{x}) \quad \text{for } x \neq 0.$$

Clearly, v is an outgoing radiating solution to the Helmholtz equation $\Delta u + k^2 u = 0$ in $\mathbb{R}^3 \setminus \{0\}$. Recalling the definition of the solution operator G_{Dir} , we obtain that $G_{Dir}(v|_{\partial D}) = \mathbf{g}^{(M_\epsilon)}$, so $\|G_{Dir}(v|_{\partial D}) - \mathbf{g}\|_{\ell^2} < \epsilon$. This completes the denseness proof of the range of G_{Dir} in ℓ^2 .

(ii) The required properties of \mathbb{G}_{Dir} follow from those of G_{Dir} and the fact that T_0 is an unitary operator in ℓ^2 and \mathcal{F}_R is an isomorphism. □

Lemma 3.6. *Let \mathbb{G}_{Dir} be given as in (3.8) and set $B_R := \{x \in \mathbb{R}^3: |x| < R\}$. For $z \in B_R$, define the function $\phi_z(\cdot) = \overline{\Phi(\cdot, z)}|_{S_R} \in L^2(S_R)$. Then $z \in D$ if and only if ϕ_z belongs to the range $\mathcal{R}(\mathbb{G}_{Dir})$ of \mathbb{G}_{Dir} .*

Proof. We first assume that $z \in D \subset B_R$. Obviously, $\Phi(\cdot, z)|_{\mathbb{R}^3 \setminus \bar{D}}$ is the unique radiating solution to the problem (1.1) with the Dirichlet data $f := \Phi(\cdot, z)|_{\partial D}$. From the definition of G_{Dir} , \mathbb{G}_{Dir} and T_1 , it follows that $G_{Dir}(f) = \mathcal{F}_R(\Phi(\cdot, z)|_{S_R})$ and

$$\mathbb{G}_{Dir}(f) = \mathcal{F}_R^{-1} T_0 G_{Dir}(f) = \mathcal{F}_R^{-1} T_0 \mathcal{F}_R \left(\Phi(\cdot, z)|_{S_R} \right) = T_1 \left(\Phi(\cdot, z)|_{S_R} \right). \tag{3.13}$$

Recalling the expansion (2.8) for the fundamental solution $\Phi(x, z)$ with $|x| > |z|$, we arrive at

$$\begin{aligned} T_1 \left(\Phi(x, z)|_{x \in S_R} \right) &= -ik \sum_{n=0}^{\infty} \sum_{m=-n}^n \overline{h_n^{(1)}(kR) j_n(k|z|) Y_n^m(\hat{z})} Y_n^m(\hat{x}) \\ &= ik \sum_{n=0}^{\infty} \sum_{m=-n}^n h_n^{(1)}(kR) j_n(k|z|) \overline{Y_n^{-m}(\hat{z})} Y_n^{-m}(\hat{x}) \\ &= \overline{\Phi(x, z)}|_{S_R}. \end{aligned} \tag{3.14}$$

Combining (3.15) and (3.16) yields $\phi_z(\cdot) = \overline{\Phi(\cdot, z)}|_{S_R} \in \mathcal{R}(\mathbb{G}_{Dir})$.

On the other hand, let $z \in \mathbb{R}^3$ and assume that $\mathbb{G}_{Dir}(f) = \phi_z$ for some $f \in H^{1/2}(\partial D)$. Since the operator T_0 is unitary on ℓ^2 , we have that $G_{Dir} = T_0^{-1} \mathcal{F}_R \mathbb{G}_{Dir}$ and $T_1^* = \mathcal{F}_R^{-1} T_0^{-1} \mathcal{F}_R$. This implies that

$$\mathcal{F}_R^{-1} G_{Dir}(f) = \mathcal{F}_R^{-1} T_0^{-1} \mathcal{F}_R \mathbb{G}_{Dir}(f) = \mathcal{F}_R^{-1} T_0^{-1} \mathcal{F}_R(\phi_z) = T_1^*(\phi_z) = \Phi(\cdot, z)|_{S_R},$$

where the last equality follows from (3.16). Therefore, it holds that $G_{Dir}(f) = \mathcal{F}_R(\Phi(\cdot, z)|_{S_R})$. Let v be the solution of the Dirichlet problem (1.1) with the boundary data f so that $G_{Dir}(f) = \mathcal{F}_R(v|_{S_R}) = \mathcal{F}_R(\Phi(\cdot, z)|_{S_R})$. Consequently, we get $v = \Phi(\cdot, z)$ in $\{x \in \mathbb{R}^3: |x| \geq R\}$ due to the uniqueness of solutions to the exterior Dirichlet problem, and therefore $v = \Phi(\cdot, z)$ in $\mathbb{R}^3 \setminus (\bar{D} \cup \{z\})$ by analytic continuation. It is impossible that $z \in \mathbb{R}^3 \setminus \bar{D}$ since v is analytic in $\mathbb{R}^3 \setminus \bar{D}$ but $\Phi(\cdot, z)$ is singular at z . On the other hand, the relation $z \in \partial D$ would lead to a contraction that $v|_{\partial D} \in H^{1/2}(\partial D)$ but $\Phi(\cdot, z)|_{\partial D} \notin H^{1/2}(\partial D)$. Hence, we have that $z \in D$, which proves the lemma. □

We now collect properties of the middle operator S from [7, lemma 1.14].

Lemma 3.7. *Assume that k^2 is not a Dirichlet eigenvalue of $-\Delta$ in D .*

- (i) The operator S is an isomorphism from the space $H^{-1/2}(\partial D)$ into $H^{1/2}(\partial D)$.
- (ii) Let S_i be defined by (3.4) with $k = i$. Then S_i is self-adjoint and coercive as an operator from $H^{-1/2}(\partial D)$ into $H^{1/2}(\partial D)$.
- (iii) $\text{Im} \langle \varphi, S\varphi \rangle < 0$ for all $\varphi \in H^{-1/2}(\partial D)$ with $\varphi \neq 0$. Here, $\langle \cdot, \cdot \rangle$ denotes the duality between $H^{1/2}(\partial D)$ and $H^{-1/2}(\partial D)$ extending the L^2 -product in $L^2(\partial D)$.
- (iv) The difference $S - S_i$ is compact from $H^{-1/2}(\partial D)$ into $H^{1/2}(\partial D)$.

Relying on lemmas 3.5, 3.6 and 3.7, we now present a sufficient and necessary computational criterion for precisely characterizing the region occupied by the scatterer, from which a uniqueness result with the full near-field measurement data taken on S_R also follows.

Theorem 3.8. Assume that k^2 is not a Dirichlet eigenvalue of $-\Delta$ in D . Let N be the near-field operator defined in (1.6) and let ϕ_z be given as in lemma 3.6. Denote by $\lambda_j \in \mathbb{C}$ the eigenvalues of the normal operator $(T_1 N)_\# := |\text{Re}(T_1 N)| + |\text{Im}(T_1 N)|$ with the corresponding normalized eigenfunctions $\psi_j \in L^2(S_R)$. Then

$$z \in D \iff \phi_z \in \mathcal{R} \left[(T_1 N)_\#^{1/2} \right] \quad (3.15)$$

$$\iff W(z) := \left[\sum_j \frac{\left| (\phi_z, \psi_j)_{L^2(S_R)} \right|^2}{|\lambda_j|} \right]^{-1} > 0. \quad (3.16)$$

Proof. The properties of \mathbb{G}_{Dir} and S shown in lemmas 3.5 (ii) and 3.7 enable us to apply the range identity of [7, theorem 2.15] to the factorization $T_1 N = -\mathbb{G}_{Dir} S^* \mathbb{G}_{Dir}^*$. As a consequence we get $\mathcal{R} \left[(T_1 N)_\#^{1/2} \right] = \mathcal{R} [\mathbb{G}_{Dir}]$. This, together with lemma 3.6, yields (3.17). The relation (3.18) follows from Picard's range criterion. \square

We now state a uniqueness result by utilizing limited aperture near-field data only.

Theorem 3.9. Assume that the sound-soft obstacle D is contained in the ball $B_R = \{x: |x| < R\}$. Let $\Gamma_R \subset S_R$ be a sub-domain of S_R and let $u(x, y)$ denote the unique scattered field corresponding to the incident point source wave $\Phi(\cdot, y)$ with $y \in \Gamma_R$. Then ∂D can be uniquely determined by the near-field data $\{u(x, y): x, y \in \Gamma_R\}$.

Proof. Suppose there is another sound-soft obstacle $\tilde{D} \subset B_R$, and denote by $\tilde{u}(x, y)$ and $\tilde{G}(x, y)$ the corresponding scattered and total fields with respect to \tilde{D} . Set $G(x, y) := u(x, y) + \Phi(x, y)$ for $x \in \mathbb{R}^3 \setminus \bar{D}$, which is the total field corresponding to the incident point source $\Phi(x, y)$ with respect to D .

Assume that $u(x, y) = \tilde{u}(x, y)$ for all $x, y \in \Gamma_R$. Since both u and \tilde{u} are analytic in a neighborhood of the sphere S_R , we get $u(x, y) = \tilde{u}(x, y)$ and thus $G(x, y) = \tilde{G}(x, y)$ for all $x \in S_R$ and $y \in \Gamma_R$. Recalling the symmetric relation $G(x, y) = G(y, x)$ and $\tilde{G}(x, y) = \tilde{G}(y, x)$, we find that $G(y, x) = \tilde{G}(y, x)$ for all $x \in S_R$ and $y \in \Gamma_R$. Again applying the analytic continuation along the sphere S_R gives that $G(x, y) = \tilde{G}(x, y)$ for all $x, y \in S_R$. This implies that $u(x, y) = \tilde{u}(x, y)$ for all $x, y \in S_R$. Finally, we obtain $\partial D = \partial \tilde{D}$ as a consequence of theorem 3.8. \square

Numerically, one may still recover ∂D from $\{u(x, y): x, y \in \Gamma_R\}$ with Γ_R defined as in theorem 3.9, based on the computational criterion presented in theorem 3.8. More precisely, introduce the near-field operator $\tilde{N}: L^2(\Gamma_R) \rightarrow L^2(\Gamma_R)$ by

$$(\tilde{N}g)(x) = \int_{\Gamma_R} u(x; y)g(y)ds(y) \quad \text{for } x \in \Gamma_R, \quad g \in L^2(\Gamma_R),$$

and define the operator $\tilde{T}_1: L^2(\Gamma_R) \rightarrow L^2(\Gamma_R)$ as

$$(\tilde{T}_1g)(x) = \int_{\Gamma_R} K(x, y)g(y)ds(y) \quad \text{for } g \in L^2(\Gamma_R)$$

with the kernel $K(x, y)$ given by (3.10). Then one can design an inversion algorithm similarly to theorem 3.8; see section 6 for the numerical examples.

3.3. An explicit example for the unit ball

Suppose $D = \{x: |x| < 1\}$ is a sound-soft ball. In this special case we can present explicit eigenvalues of T_1N and compute the series appearing in (3.18). Since the fundamental solution $\Phi(x, y)$ with $|x| < |y|$ admits the expansion (2.8), the scattered field $u(x, y)$, generated by the incident point source wave $\Phi(\cdot, y)$ with $|y| = R > 1$, is of the form

$$u(x, y) = -ik \sum_{n=0}^{\infty} \sum_{m=-n}^n h_n^{(1)}(k|y|) \overline{Y_n^m(\hat{y})} \frac{j_n(k)}{h_n^{(1)}(k)} h_n^{(1)}(k|x|) Y_n^m(\hat{x}), \quad |x| > 1.$$

Let $g \in L^2(S_R)$ be given by (2.1) with the Fourier coefficients $g_{n,m}$. By the definition of the near-field operator N , we have that for $x \in S_R$,

$$(Ng)(x) = \int_{S_R} u(x, y)g(y)ds(y) = -ikR^2 \sum_{n=0}^{\infty} \sum_{m=-n}^n h_n^{(1)}(kR)^2 \frac{j_n(k)}{h_n^{(1)}(k)} Y_n^m(\hat{x}) g_{n,m}.$$

Then, by (3.12) it holds that

$$T_1N(g) = ikR^2 \sum_{n=0}^{\infty} \sum_{m=-n}^n \left| h_n^{(1)}(kR) \right|^2 \frac{j_n(k)}{h_n^{(1)}(k)} Y_n^m(\hat{x}) g_{n,m}.$$

This implies that the eigenvalues λ_n and the corresponding eigenfunctions $\psi_{n,m}$ are given, respectively, by

$$\lambda_n = ikR^2 \left| h_n^{(1)}(kR) \right|^2 \frac{j_n(k)}{h_n^{(1)}(k)}, \quad \psi_{n,m}(\hat{x}) = Y_n^m(\hat{x}),$$

for $n = 0, 1, \dots$ and $m = -n, \dots, n$. Note that the multiplicity of λ_n is $2n + 1$. Using again the expansion of $\Phi(x, z)$ with $x \in S_R$, $|z| < R$, it is seen that

$$\phi_z(\hat{x}) = \overline{\Phi(x, z)} \Big|_{x \in S_R} = -ik \sum_{n=0}^{\infty} \sum_{m=-n}^n \overline{h_n^{(1)}(kR) Y_n^m(\hat{x})} j_n(k|z|) \overline{Y_n^m(\hat{z})} \quad \text{for } |z| < R.$$

Therefore, by the additional theorem,

$$\begin{aligned} \sum_{m=-n}^n \left| \left(\phi_z, \psi_{n,m} \right)_{L^2(S_R)} \right|^2 &= \left| \overline{kh_n^{(1)}(kR) j_n(k|z|) R^2} \right|^2 \sum_{m=-n}^n \left| \overline{Y_n^m(\hat{z})} \right|^2 \\ &= \left| \overline{kh_n^{(1)}(kR) j_n(k|z|) R^2} \right|^2 \frac{2n + 1}{4\pi}. \end{aligned}$$

This, together with the asymptotic behavior of Hankel functions, yields

$$\begin{aligned} \sum_{n=0}^{\infty} \sum_{m=-n}^n \frac{\left| \left(\phi_z, \psi_{n,m} \right)_{L^2(S_R)} \right|^2}{|\lambda_n|} &= \sum_{n=0}^{\infty} \frac{1}{|\lambda_n|} \sum_{m=-n}^n \left| \left(\phi_z, \psi_{n,m} \right)_{L^2(S_R)} \right|^2 \\ &= \sum_{n=0}^{\infty} \frac{k(2n+1)R^4}{4\pi R^2} \frac{|j_n(k|z|)|^2}{|j_n(k)|} |h_n^{(1)}(k)| \\ &= \frac{R^2}{4\pi} \sum_{n=0}^{\infty} |z|^{2n} \left(1 + \mathcal{O}\left(\frac{1}{n}\right) \right), \end{aligned}$$

which is convergent if and only if $|z| < 1$. This implies that the indicator function $W(z) > 0$ if and only if $z \in D$.

4. Impedance boundary condition

In this section, we prove that the factorization of T_1N is applicable to the case of impedance boundary conditions:

$$\mathcal{B}u := \frac{\partial u}{\partial \nu} + \rho(x)u = f \quad \text{on } \partial D,$$

where the impedance function $\rho(x) \in L^\infty(\partial D)$ is complex-valued and satisfies that $\text{Im}(\rho) \geq 0$ almost everywhere on ∂D . To this end, we introduce the incidence operator $H_{\text{imp}}: \ell^2 \rightarrow H^{-1/2}(\partial D)$ by (see (3.1) in the case of Dirichlet boundary conditions)

$$\left(H_{\text{imp}} \mathbf{g} \right)(x) := ikR^2 \sum_{n=0}^{\infty} \sum_{m=-n}^n h_n^{(1)}(kR) g_{n,m} \left(\frac{\partial}{\partial \nu(x)} + \rho(x) \right) \left[j_n(k|x|) Y_n^m(\hat{x}) \right], \quad x \in \partial D \quad (4.1)$$

with $\mathbf{g} \in \ell^2$ given by (2.1). Further, we define the solution operator $G_{\text{imp}}: H^{-1/2}(\partial D) \rightarrow \ell^2$ by

$$G_{\text{imp}}(f) = \left\{ b_n^m h_n^{(1)}(kR) : n = 0, 1, \dots, m = -n, \dots, n \right\},$$

where $b_n^m h_n^{(1)}(kR)$ are the Fourier coefficients of $u|_{S_R}$ with u the unique radiating solution to the problem (1.1) under the impedance boundary condition.

Define the layer-potential operators K , K' and J , respectively, by

$$\begin{aligned} K\varphi(x) &= \int_{\partial D} \frac{\partial \Phi(x, y)}{\partial \nu(y)} \varphi(y) ds(y) \quad \text{for } x \in \partial D, \\ K'\varphi(x) &= \int_{\partial D} \frac{\partial \Phi(x, y)}{\partial \nu(x)} \varphi(y) ds(y) \quad \text{for } x \in \partial D, \\ J\varphi(x) &= \frac{\partial}{\partial \nu(x)} \int_{\partial D} \frac{\partial \Phi(x, y)}{\partial \nu(y)} \varphi(y) ds(y) \quad \text{for } x \in \partial D. \end{aligned} \quad (4.2)$$

It follows from [9] that the operators $K: H^{1/2}(\partial D) \rightarrow H^{1/2}(\partial D)$, $K': H^{-1/2}(\partial D) \rightarrow H^{-1/2}(\partial D)$ and $J: H^{1/2}(\partial D) \rightarrow H^{-1/2}(\partial D)$ are all bounded.

Theorem 4.1. Let T_0 , T_1 and \mathcal{N} be given by (3.6), (3.13) and (2.6), respectively. Then

$$T_0 \mathcal{N} = -R^2 (T_0 G_{\text{imp}}) T_{\text{imp}}^* (T_0 G_{\text{imp}})^*, \tag{4.3}$$

$$T_1 N = -\mathbb{G}_{\text{imp}} T_{\text{imp}}^* \mathbb{G}_{\text{imp}}^*, \quad \mathbb{G}_{\text{imp}} := \mathcal{F}_R^{-1} T_0 G_{\text{imp}}, \tag{4.4}$$

where $T_{\text{imp}}: H^{1/2}(\partial D) \rightarrow H^{-1/2}(\partial D)$ is defined as $T_{\text{imp}} = J + i(\text{Im } \rho)I + K' \bar{\rho} + \rho K + \rho S \bar{\rho}$.

Proof. From (3.1) and (4.1), it is deduced that the adjoint operator $H_{\text{imp}}^*: H^{1/2}(\partial D) \rightarrow \ell^2$ takes the form

$$H_{\text{imp}}^*(\varphi) = \left\{ -ikR^2 \overline{h_n^{(1)}(kR)} \int_{\partial D} \left(\frac{\partial}{\partial \nu(y)} + \overline{\rho(y)} \right) \left[j_n(k|y|) \overline{Y_n^m(\hat{y})} \right] \varphi(y) ds(y) \right\}_{n,m} \tag{4.5}$$

for all $\varphi \in H^{1/2}(\partial D)$. Define

$$V(x) := \int_{\partial D} \left[\frac{\partial \Phi(x, y)}{\partial \nu(y)} + \overline{\rho(y)} \Phi(x, y) \right] \varphi(y) ds(y), \quad x \in \mathbb{R}^3 \setminus \partial D.$$

It is seen from (2.8) that on $|x| = R$,

$$V(x) \Big|_{S_R} = ik \sum_{n=0}^{\infty} \sum_{m=-n}^n h_n^{(1)}(kR) Y_n^m(\hat{x}) \int_{\partial D} \left(\frac{\partial}{\partial \nu(y)} + \overline{\rho(y)} \right) \left[j_n(k|y|) \overline{Y_n^m(\hat{y})} \right] \varphi(y) ds(y).$$

This, together with (4.5), implies that

$$R^2 T_0 G_{\text{imp}} (\mathcal{B}V|_{\partial D}) = H_{\text{imp}}^* \varphi. \tag{4.6}$$

Using the jump relations of layer-potentials, we have

$$(\mathcal{B}V)|_{\partial D} = J\varphi + i(\text{Im } \rho)\varphi + K'(\bar{\rho}\varphi) + \rho K\varphi + \rho S(\bar{\rho}\varphi) = T_{\text{imp}}\varphi.$$

Then, by (4.6) we have

$$R^2 T_0 G_{\text{imp}} T_{\text{imp}} = H_{\text{imp}}^* \quad \text{or} \quad R^2 T_{\text{imp}}^* G_{\text{imp}}^* T_0^* = H_{\text{imp}}. \tag{4.7}$$

Recalling the definition of the operator \mathcal{N} in (2.7), we observe that $\mathcal{N} = -G_{\text{imp}} H_{\text{imp}}$ under the impedance boundary condition, from which the relation

$$T_0 \mathcal{N} = -R^2 (T_0 G_{\text{imp}}) T_{\text{imp}}^* (T_0 G_{\text{imp}})^*$$

follows. This completes the Proof of (4.3). Since $N = \mathcal{F}_R^{-1} \mathcal{N} \mathcal{F}_R$, the factorization (4.4) can be justified in the same manner as in the case of Dirichlet boundary conditions. \square

Theorem 4.2. Assume that k^2 is not an eigenvalue of $-\Delta$ in D with respect to the impedance boundary condition.

- (i) The operator \mathbb{G}_{imp} is compact, one-to-one with a dense range in $L^2(S_R)$.
- (ii) The operator T_{imp} is an isomorphism from the space $H^{1/2}(\partial D)$ into $H^{-1/2}(\partial D)$.
- (iii) Let J_i be defined by (4.2) with $k = i$. Then J_i is self-adjoint and coercive as an operator from $H^{1/2}(\partial D)$ into $H^{-1/2}(\partial D)$.
- (iv) $\text{Im} \langle T_{\text{imp}} \varphi, \varphi \rangle > 0$ for all $\varphi \in H^{-1/2}(\partial D)$ with $\varphi \neq 0$.
- (v) The difference $T_{\text{imp}} - J_i$ is compact from $H^{1/2}(\partial D)$ into $H^{-1/2}(\partial D)$.

Proof. We only prove the first assertion (i). The Proof of the other assertions (ii)–(v) can be seen in [7]. Since the operator \mathcal{F}_R is an isomorphism, the operator \mathbb{G}_{imp} can be rewritten as

$$\mathbb{G}_{\text{imp}} = \left(\mathcal{F}_R^{-1} T_0 \mathcal{F}_R \right) \mathcal{F}_R^{-1} G_{\text{imp}} =: T_1 G_2, \quad G_2 := \mathcal{F}_R^{-1} G_{\text{imp}}.$$

By the definition of G_{imp} , the operator $G_2: H^{-1/2}(\partial D) \rightarrow L^2(S_R)$ maps the boundary data f into the restriction to S_R of the solution of the problem (1.1). Therefore, it is sufficient to prove that G_2 is compact, one-to-one with a dense range in $L^2(S_R)$ since T_1 is an isomorphism.

Clearly, the compactness and injectivity follow easily from the well-posedness of the scattering problem and analytic continuation arguments. To prove the denseness of the range $\mathcal{R}(\mathbb{G}_{\text{imp}})$, we only need to show that the adjoint operator $G_2^*: L^2(S_R) \rightarrow H^{1/2}(\partial D)$ is injective. To this end, let u and w be the solutions to the problem (1.1) with the impedance boundary condition $\mathcal{B}u = f$ and $\mathcal{B}w = -\mathcal{B}w^i$, respectively, where $f \in H^{-1/2}(\partial D)$ and

$$w^i(x) = 2 \int_{S_R} \Phi(x; y) \overline{\varphi(y)} ds(y) \quad \text{for } x \in \mathbb{R}^3 \setminus S_R, \quad \varphi \in L^2(S_R).$$

Since w^i , u and w satisfy the Sommerfeld radiation condition, by applying Green's second theorem we see that

$$\int_{\partial D} \left[\frac{\partial w}{\partial \nu} u - w \frac{\partial u}{\partial \nu} \right] ds = 0, \quad \int_{S_R} \left[\frac{\partial w^i}{\partial \nu} \Big|_+ u - w^i \frac{\partial u}{\partial \nu} \Big|_+ \right] ds = 0. \quad (4.8)$$

Here, the subscripts $|_{\pm}$ denote the limits taken from outside and inside of S_R , respectively. Again applying Green's formula, recalling the jump relation for the single-layer potentials and using (4.8) and the impedance boundary condition for $w^t := w + w^i$, we obtain that

$$\begin{aligned} (G_2^* f, \varphi)_{L^2(S_R)} &= \int_{S_R} u \overline{\varphi} ds \\ &= \int_{S_R} u \left[\frac{\partial w^i}{\partial \nu} \Big|_- - \frac{\partial w^i}{\partial \nu} \Big|_+ \right] ds \\ &= \int_{S_R} \left[u \frac{\partial w^i}{\partial \nu} \Big|_- - \frac{\partial u}{\partial \nu} w^i \right] ds + \int_{S_R} \left[\frac{\partial u}{\partial \nu} w^i - u \frac{\partial w^i}{\partial \nu} \Big|_+ \right] ds \\ &= \int_{S_R} \left[u \frac{\partial w^i}{\partial \nu} \Big|_- - \frac{\partial u}{\partial \nu} w^i \right] ds \\ &= \int_{\partial D} \left(\frac{\partial w^i}{\partial \nu} u - w^i \frac{\partial u}{\partial \nu} \right) ds + \int_{\partial D} \left(\frac{\partial w}{\partial \nu} u - w \frac{\partial u}{\partial \nu} \right) ds \\ &= \int_{\partial D} \left[\mathcal{B}(w^t) u - w^t \mathcal{B}u \right] ds \\ &= -\langle f, \overline{w^t} \rangle_{H^{-1/2}(\partial D) \times H^{1/2}(\partial D)}. \end{aligned}$$

This implies that $G_2^* \varphi = -\overline{w^t}|_{\partial D}$. Let $G_2^* \varphi = 0$. We then have $w^t|_{\partial D} = 0$ so, by the impedance boundary condition, $(\partial w^t / \partial \nu)|_{\partial D} = 0$. Thus we get $w^t = 0$ in $B_R \setminus D$, which, together with Holmgren's uniqueness theorem and the uniqueness result for the exterior Dirichlet problem, implies that $w^t = 0$ in $\mathbb{R}^3 \setminus B_R$. Finally, using the jump relation of the layer potentials gives

$$0 = \frac{\partial w^t}{\partial \nu} \Big|_- - \frac{\partial w^t}{\partial \nu} \Big|_+ = \frac{\partial w^i}{\partial \nu} \Big|_- - \frac{\partial w^i}{\partial \nu} \Big|_+ = \bar{\varphi}.$$

Hence, G_2^* is injective and G_2 has a dense range in $L^2(S_R)$. □

Similarly to theorem 3.8 for the Dirichlet case, one can prove the following result.

Theorem 4.3. Assume that k^2 is not an eigenvalue of $-\Delta$ in D with respect to the impedance boundary condition. For $z \in B_R$, define the function $\phi_z(\cdot) = \Phi(\cdot, z)|_{S_R}$. Then

$$z \in D \iff \phi_z \in \mathcal{R} \left[(T_1 N)_\#^{1/2} \right]$$

$$\iff W(z) := \left[\sum_j \frac{\left| (\phi_z, \psi_j)_{L^2(S_R)} \right|^2}{\lambda_j} \right]^{-1} > 0,$$

where $\lambda_j \in \mathbb{C}$ are the eigenvalues of the normal operator $(T_1 N)_\# := |\operatorname{Re}(T_1 N)| + |\operatorname{Im}(T_1 N)|$ with the corresponding normalized eigenfunctions $\psi_j \in L^2(S_R)$.

Remark 4.4. The factorization method with near-field data extends straightforwardly to the case $\rho(x) = 0$, that is, the Neumann boundary condition, provided k^2 is not a Neumann eigenvalue of $-\Delta$ in D . Moreover, one can also apply theorem 4.3 to complex obstacles with the generalized impedance boundary condition $\mathcal{B}u = \partial u / \partial \nu + \operatorname{div}_{\partial D}(\mu \nabla_{\partial D} u) + \rho u$ on ∂D . To achieve this, one needs to combine the Proof of theorem 4.3 with the arguments from [12], where the factorization method with far-field patterns of all incident plane waves was justified.

5. Inverse medium scattering problem

In this section we assume that D is a penetrable obstacle with the refraction index $n(x)$ satisfying that $\operatorname{Re}(n) \geq 0, \operatorname{Im}(n) \geq 0, n \neq 1$ in D and $n \equiv 1$ in $\mathbb{R}^3 \setminus \bar{D}$. Then the scattering solution u solves the equation

$$\Delta u + k^2 n(x) u = k^2 (1 - n(x)) f, \quad \text{in } \mathbb{R}^3,$$

with $f = u^i|_D \in L^2(D)$, where $u^i(\cdot) = \Phi(\cdot, y)$ is the incident point source at $y \in S_R$. For medium scattering problems, the solution operator $G_{pen}: L^2(D) \rightarrow \ell^2$ and the incidence operator $H_{pen}: \ell^2 \rightarrow L^2(D)$ are defined as follows:

$$G_{pen}(f) = \left\{ b_n^m h_n^{(1)}(kR) : n \in \mathbb{N}, m = -n, \dots, n \right\}, \tag{5.9}$$

$$H_{pen}(\mathbf{g}) = ikR^2 \sum_{n=0}^{\infty} \sum_{m=-n}^n h_n^{(1)}(kR) g_{n,m} u_{n,m}^i(x), \quad x \in D, \tag{5.10}$$

where $b_n^m h_n^{(1)}(kR)$ are the Fourier coefficients of $u|_{S_R}$, and $u_{n,m}^i, \mathbf{g}$ are given as in section 2.

From (5.10) it is easily seen that the adjoint operator $H_{pen}^*: L^2(D) \rightarrow \ell^2$ is given by

$$H_{pen}^* \varphi = \left\{ -ikR^2 \overline{h_n^{(1)}(kR)} \int_D j_n(k|x|) \overline{Y_n^m(\hat{x})} \varphi(x) dx: n \in \mathbb{N}, m = -n, \dots, n \right\}.$$

This, together with the unitary operator T_0 and the expansion (2.9), implies that

$$(T_0^* H_{pen}^* \varphi)(x) = R^2 \mathcal{F}_R \left(\int_D \Phi(x, y) \varphi(y) dy \Big|_{S_R} \right). \quad (5.11)$$

For penetrable obstacles, define the operator $T_{pen}: L^2(D) \rightarrow L^2(D)$ by

$$T_{pen} \varphi = \frac{1}{k^2(n-1)} \varphi - \int_D \Phi(x, y) \varphi(y) dy, \quad x \in D.$$

Then one can derive from (5.9) and (5.11) that $T_0^* H_{pen}^* = R^2 G_{pen} T_{pen}$ or $H_{pen} T_0 = R^2 T_{pen}^* G_{pen}^*$. Therefore, we have the factorization

$$\begin{aligned} T_0 \mathcal{N} &= -R^2 (T_0 G_{pen}) T_{pen}^* (T_0 G_{pen})^*, \\ T_1 N &= -G_{pen} T_{pen}^* G_{pen}^*, \quad G_{pen} := \mathcal{F}_R^{-1} T_0 G_{pen}. \end{aligned} \quad (5.12)$$

Here, \mathcal{N} and T_1 are defined as in (2.6) and (3.10), respectively.

It is known from [5] that the middle operator T_{pen} of the factorization (5.12) satisfies all the properties of the range identity [7, theorem 2.15] provided $n(x) \neq 1$ for all $x \in D$ and k^2 is not an interior transmission eigenvalue in D . We thus have the following result.

Theorem 5.1. *Let $n(x) \neq 1$ for all $x \in D$ and assume that k^2 is not an interior transmission eigenvalue in D . Define $\phi_z(\cdot) = \overline{\Phi(\cdot, z)}|_{S_R}$ with $z \in B_R$. Then*

$$\begin{aligned} z \in D &\iff \phi_z \in \mathcal{R} \left[(T_1 N)_\#^{1/2} \right] \\ &\iff W(z) := \left[\sum_j \frac{\left| (\phi_z, \psi_j)_{L^2(S_R)} \right|^2}{\lambda_j} \right]^{-1} > 0, \end{aligned}$$

where $\lambda_j \in \mathbb{C}$ are the eigenvalues of the normal operator $(T_1 N)_\# := |\operatorname{Re}(T_1 N)| + |\operatorname{Im}(T_1 N)|$ with the corresponding normalized eigenfunctions $\psi_j \in L^2(S_R)$.

6. Numerical results

In this section, we present several numerical examples which are all done in \mathbb{R}^2 to illustrate our inversion algorithm; as remarked in the introduction, the theoretical results are also valid for the two-dimensional case.

We first discuss briefly how to discretize the outgoing-to-incoming operator T_1 in two dimensions. By employing the polar coordinates we write $x = (r, \theta_x)$ for $x \in \mathbb{R}^2$. The two-dimensional fundamental solution to the Helmholtz equation is of the form

$$\Phi(x, y) = \frac{i}{4} H_0^{(1)}(k|x-y|), \quad x \neq y.$$

In particular, for $|x| > |y|$ there holds the expansion

$$\Phi(x, y) = \frac{i}{4} \sum_{-\infty}^{+\infty} H_n^{(1)}(k|x|) j_n(k|y|) e^{in(\theta_x - \theta_y)}. \quad (6.1)$$

Note that $H_n^{(1)}$ are Hankel functions of the first kind of order n . The two-dimensional outgoing-to-incoming operator T_1 can be represented as (see (3.12) for the 3D case)

$$(T_1\varphi)(R, \theta_x) = - \sum_{-\infty}^{+\infty} \left(\frac{\overline{H_n^{(1)}(kR)}}{H_n^{(1)}(kR)} \varphi_n \right) \frac{e^{in\theta_x}}{\sqrt{2\pi}}, \quad \varphi_n = \frac{1}{R} \int_{S_R} \varphi(x) \frac{e^{-in\theta_x}}{\sqrt{2\pi}} ds(x). \quad (6.2)$$

where $\{e^{in\theta_x}/\sqrt{2\pi}, \theta_x \in [0, 2\pi]: n \in \mathbb{Z}\}$ forms a complete orthonormal system in $L^2(\mathbb{S}^1)$. By arguing similarly as in the proof of (3.9), we have

$$(T_1\varphi)(x) = \int_{S_R} K(x, y)\varphi(y) ds(y) \quad \text{for } \varphi \in L^2(S_R)$$

with the kernel given by

$$K(x, y) := - \frac{1}{2\pi R} \sum_{-\infty}^{\infty} \left(\frac{\overline{H_n^{(1)}(kR)}}{H_n^{(1)}(kR)} \right) e^{in(\theta_x - \theta_y)}.$$

In our numerical implementation, the operator T_1 is approximated by the truncated operator

$$(T_{1, M_1}\varphi)(x) = \int_{S_R} K_{M_1}(x, y)\varphi(y) ds(y) \quad \text{for } \varphi \in L^2(S_R),$$

with some $M_1 \in \mathbb{Z}$ and the kernel given by

$$K_{M_1}(x, y) := - \frac{1}{2\pi R} \sum_{-M_1}^{M_1} \left(\frac{\overline{H_n^{(1)}(kR)}}{H_n^{(1)}(kR)} \right) e^{in(\theta_x - \theta_y)}.$$

Remark 6.1. It is pointed out that $T_{1, M_1}N$ is indeed convergent to T_1N as $M_1 \rightarrow \infty$. Choose $0 < R_0 < R$ such that $D \subset B_{R_0}$. For a given $g \in L^2(S_R)$ define $U(x) := \int_{S_R} u(x, y)g(y) ds(y)$ for $x \in \mathbb{R}^2 \setminus \overline{D}$ and $\varphi := Ng = U|_{S_R}$. By the integral representation formula, we obtain that

$$U(x) = \int_{\partial B_{R_0}} \left(U(y) \frac{\partial \Phi(x, y)}{\partial \nu(y)} - \frac{\partial U}{\partial \nu}(y) \Phi(x, y) \right) ds(y)$$

Applying the expansion (6.1) gives

$$\varphi_n = \frac{i\sqrt{2\pi}}{4} H_n^{(1)}(kR) J_n(kR_0) \int_{\partial B_{R_0}} \left(U(y) \frac{\partial e^{-in\theta_y}}{\partial \nu(y)} - \frac{\partial U}{\partial \nu}(y) e^{-in\theta_y} \right) ds(y)$$

Using the asymptotic behavior of the Hankel and Bessel functions (see, e.g., [2, pp 73–74]), it can be seen that

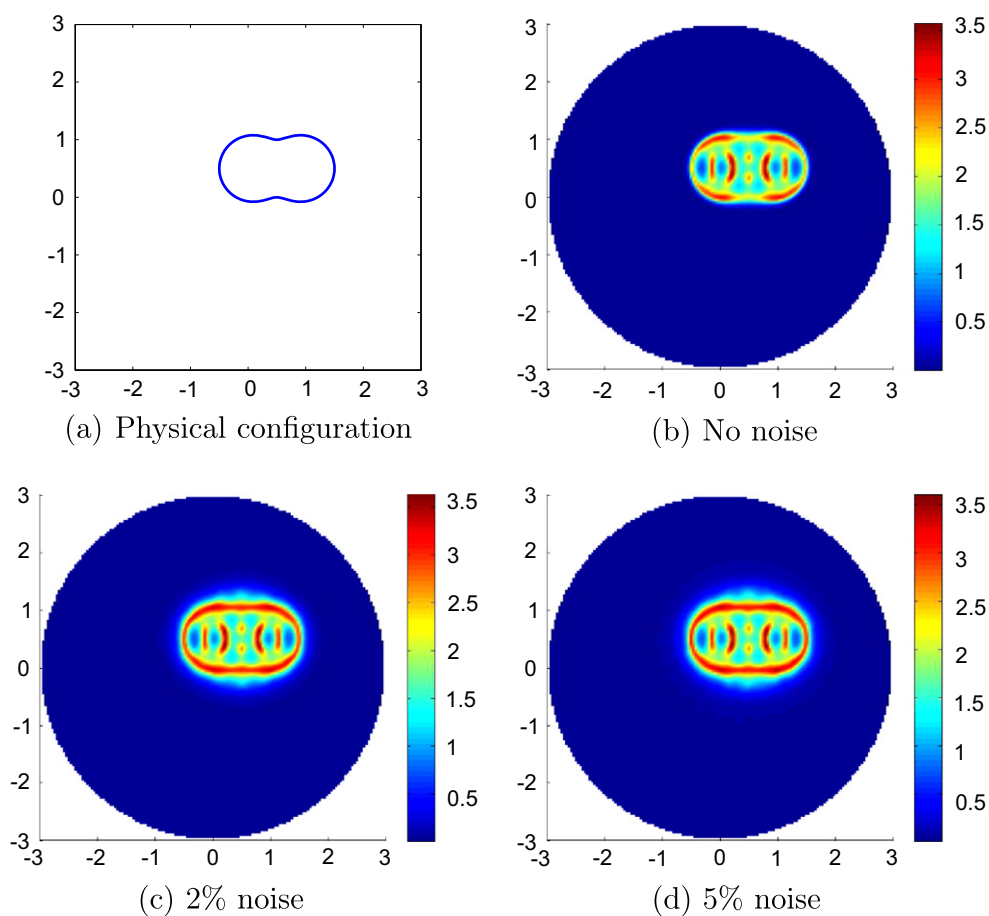


Figure 1. Reconstruction of a peanut-shaped, sound-soft obstacle. Near-field data are taken on $\{x: |x| = 3\}$.

Table 1. Parametrization of the obstacles to be reconstructed, where the parameters $c_j \in \mathbb{R}$.

Obstacle type	Parametrization:
Apple shaped	$x(t) = (c_1, c_2) + \frac{0.5 + 0.4 \cos t + 0.1 \sin(2t)}{1 + 0.7 \cos t} (\cos t, \sin t), t \in [0, 2\pi]$
Kite shaped	$x(t) = (c_1, c_2) + (\cos t + 0.65 \cos(2t) - 0.65, 1.5 \sin t), t \in [0, 2\pi]$
Peanut shaped	$x(t) = (c_1, c_2) + \sqrt{\cos^2 t + 0.25 \sin^2 t} (\cos t, \sin t), t \in [0, 2\pi]$
Rounded triangle	$x(t) = (c_1, c_2) + (2 + 0.3 \cos(3t)) (\cos t, \sin t), t \in [0, 2\pi]$

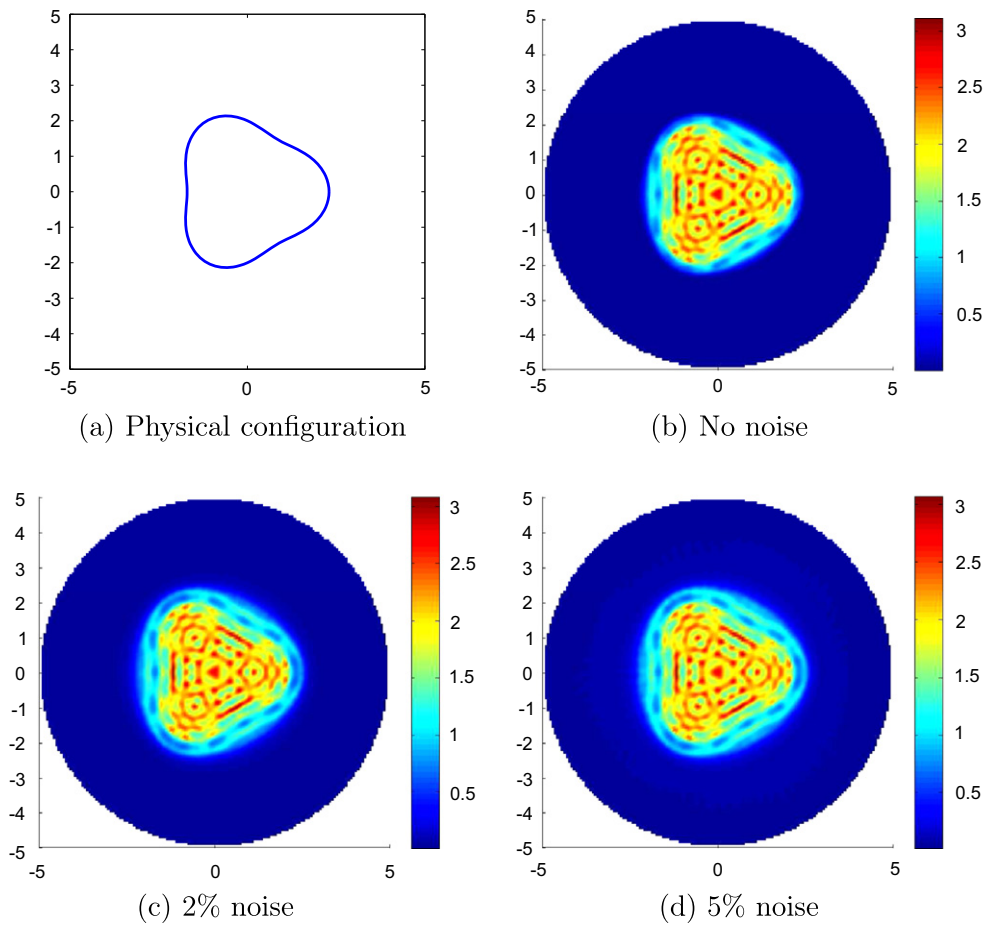


Figure 2. Reconstruction of a rounded triangle-shaped, sound-hard obstacle. Near-field data are taken on $\{x: |x| = 5\}$.

$$H_n^{(1)}(kR)J_n(kR_0) = \frac{1}{|n|\pi i} \left(\frac{R_0}{R}\right)^{|n|} \left(1 + O\left(\frac{1}{|n|}\right)\right), \quad |n| \rightarrow \infty$$

$$\frac{\overline{H_n^{(1)}(kR)}}{H_n^{(1)}(kR)} = -1 + O\left(\frac{1}{|n|}\right), \quad |n| \rightarrow \infty.$$

This leads to the result that

$$\begin{aligned} \|T_1\varphi - T_{1,M_1}\varphi\|_{L^2(B_R)} &\leq C \|T_1\varphi - T_{1,M_1}\varphi\|_{L^\infty(B_R)} \\ &\leq C \sum_{|n|>M_1} \frac{1}{|n|} \left(\frac{R_0}{R}\right)^{|n|} \left(\|U\|_{L^2(\partial B_{R_0})} + \left\| \frac{\partial U}{\partial \nu} \right\|_{L^2(\partial B_{R_0})} \right) \\ &\leq C \left(\frac{R_0}{R}\right)^{M_1+1} \|g\|_{L^2(B_R)} \end{aligned}$$

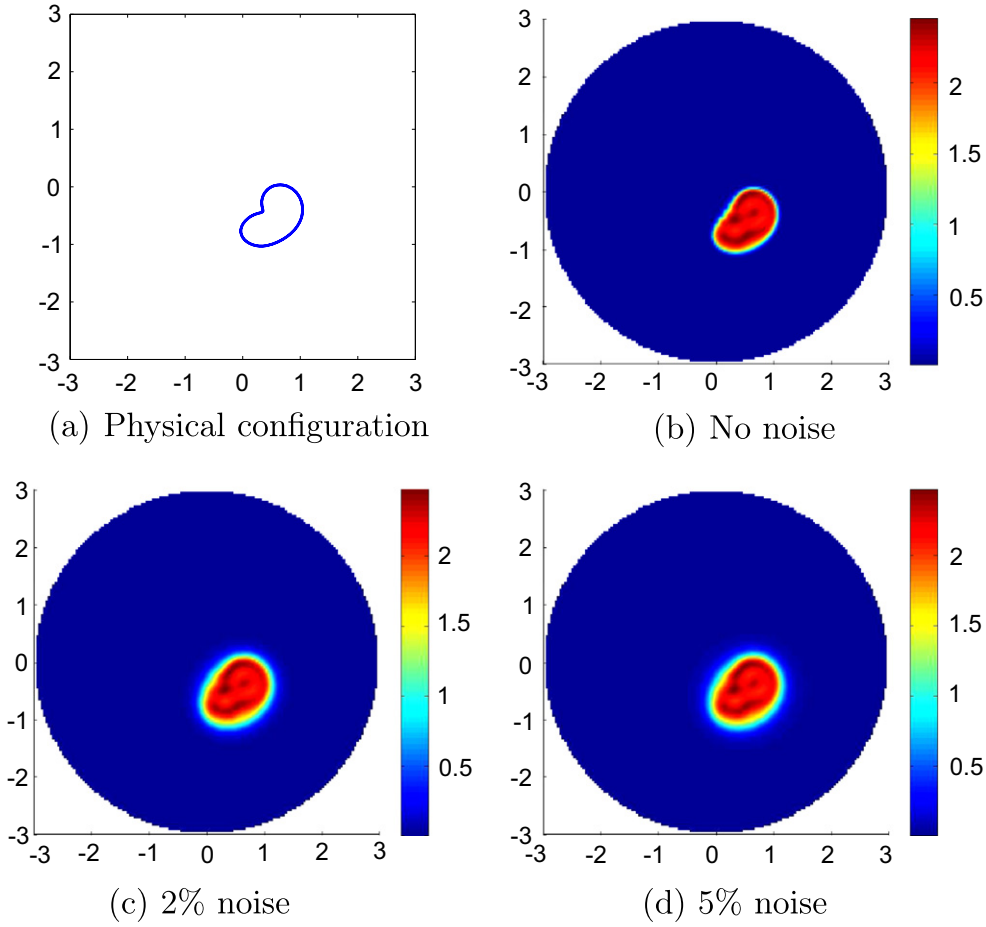


Figure 3. Reconstruction of an apple-shaped, impenetrable obstacle of impedance-type. Near-field data are taken on $\{x: |x| = 3\}$.

This means that for any $g \in L^2(B_R)$,

$$\|T_1 N g - T_{1, M_1} N g\|_{L^2(B_R)} \leq C \left(\frac{R_0}{R}\right)^{M_1+1} \|g\|_{L^2(B_R)}.$$

Thus, we conclude that $T_1 N$ rapidly converges to $T_{1, M_1} N$ in $L^2(B_R)$ as $M_1 \rightarrow \infty$. In this section, we choose $M_1 = 100$, which is large enough for all the numerical examples below.

To discretize the near-field operator N , we take the scattered field at a uniformly distributed grid over S_R with the step size $\Delta\theta_x = \Delta\theta_y = \pi/M$ for some $M \in \mathbb{N}$, that is,

$$\theta_x = \theta_x(j) = \frac{(j-1)\pi}{M}, \quad \theta_y = \theta_y(j) = \frac{(j-1)\pi}{M}, \quad j = 1, 2, \dots, 2M.$$

Define the set $\mathcal{K} := \{j \in \mathbb{N}: 1 \leq j \leq 2M\}$. Then we have the near-field matrix

$$\mathbf{N}_{2M \times 2M} = \left[u(R, \theta_x(p); R, \theta_y(q)) \right]_{p, q \in \mathcal{K}}, \quad (6.3)$$

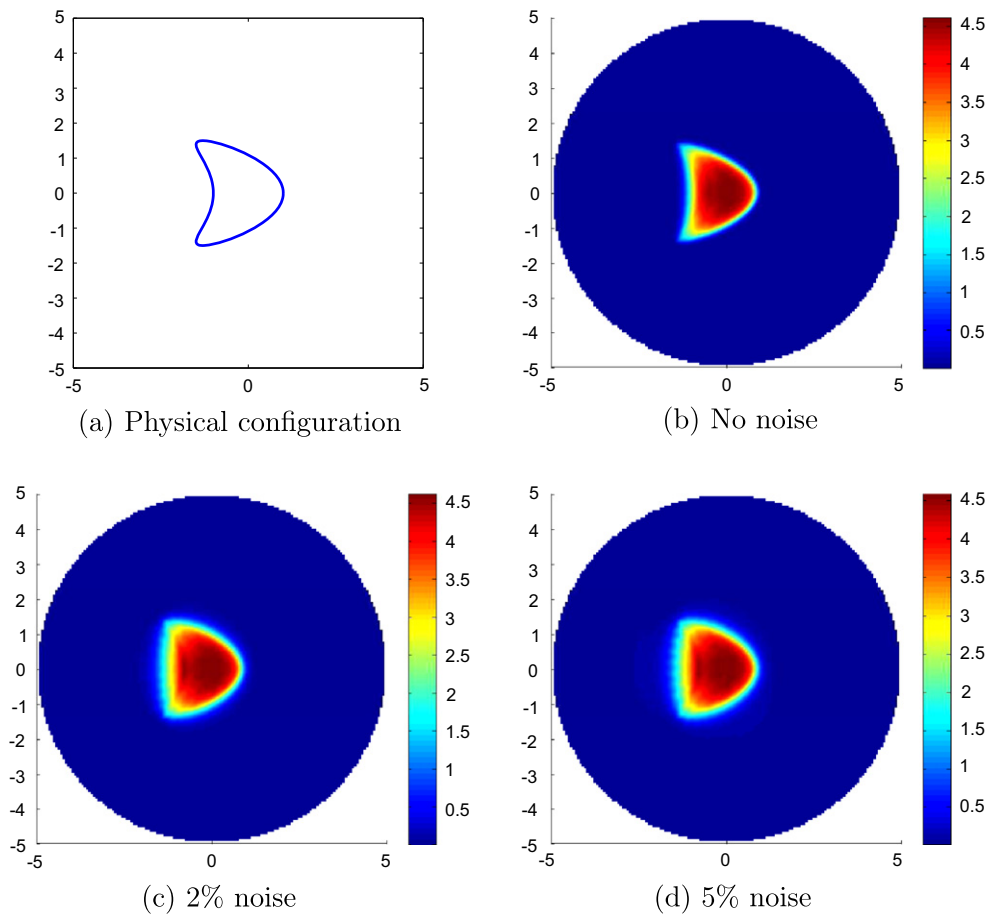


Figure 4. Reconstruction of a kite-shaped, penetrable obstacle. Near-field data are taken on $\{x: |x| = 5\}$.

and the finite-dimensional matrix $\mathbf{T}_{1,2M \times 2M} = \left[K_{M_1}(R, \theta_x(p); R, \theta_y(q)) \right]_{p,q \in \mathcal{K}}$ for the discretization of T_1 . Let $\mathbf{N}_{2M \times 2M}^{1,s} := \mathbf{T}_{1,2M \times 2M} \mathbf{N}_{2M \times 2M}$ and

$$W_M(z) := \left[\sum_{j=1}^{2M} \frac{\left| (\phi_z, \psi_j)_{L^2(S_R)} \right|^2}{\lambda_j} \right]^{-1} \quad \text{for } z \in \Omega_R, \quad (6.4)$$

where $\phi_z = \overline{\Phi(\cdot, z)}|_{S_R}$ and $\{\psi_j, \lambda_j\}_{j=1}^{2M}$ is an eigensystem of the matrix $\mathbf{N}_{2M \times 2M}^{1,s} := |\operatorname{Re}(\mathbf{N}_{2M \times 2M}^{1,s})| + |\operatorname{Im}(\mathbf{N}_{2M \times 2M}^{1,s})|$. It is expected that if M is taken large enough, the series in (6.4) approximates the true value of $W(z)$ and thus, by theorem 3.8, $W_M(z)$ should be very small in $B_R \setminus \overline{D}$ and considerably large in D .

In what follows, we present the numerical results for recovering impenetrable obstacles under the Dirichlet, Neumann or impedance boundary conditions as well as the shape and location of a penetrable medium with a constant refractive index $n \equiv n_0$ (that is, the material in D is homogeneous with the wave number $k_1^2 = k^2 n_0$). Unless otherwise stated, we always

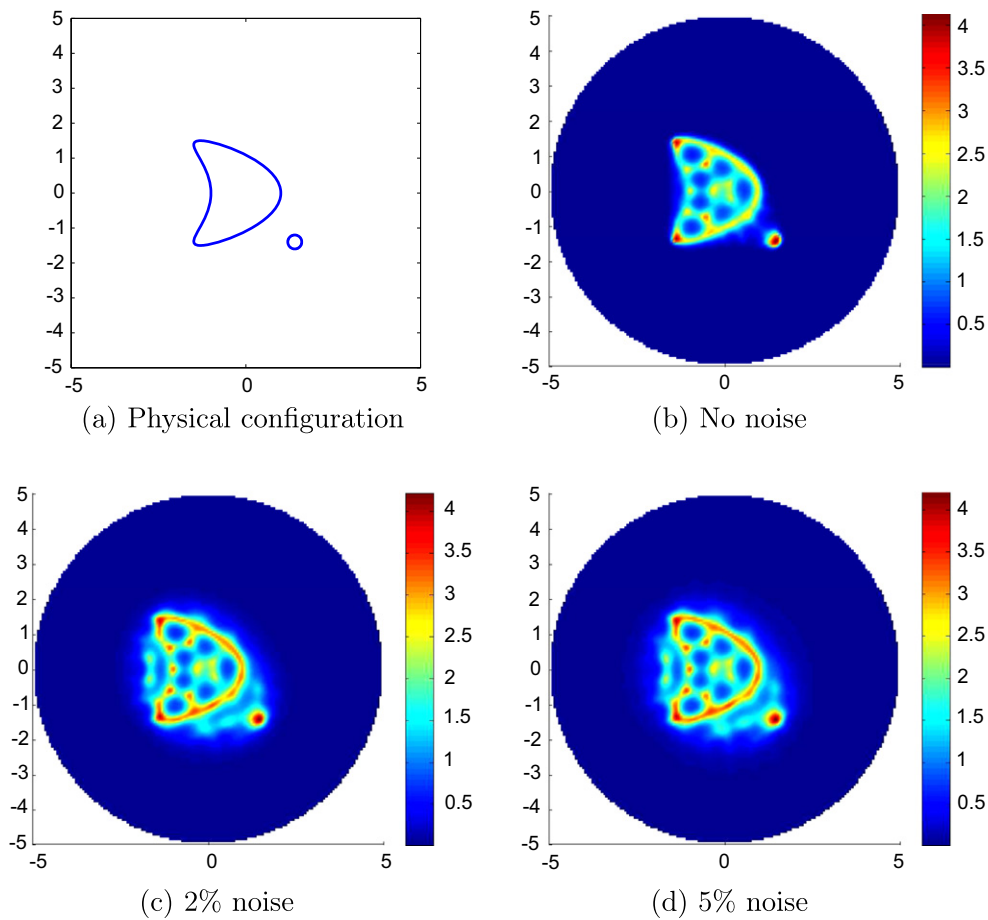


Figure 5. Reconstruction of two sound-soft obstacles of different scales: a large-scale kite-shaped one, and a small-scale circle-shaped one with radius 0.2 and centered at $(1.4, -1.4)$. The wave number $k = 5$, so the wavelength is $\lambda \approx 1.257$. The distance between the two obstacles is approximately 0.8. Near-field data are taken on $\{x: |x| = 5\}$.

set $M = 64$, $k = 10$ and plot the function $W_M(z)$ against the sampling point z . The wavelength is thus given as $\lambda = 2\pi/k = 0.628$. Recall that the sphere S_R with $R > 0$ denotes the position where the near-field is measured. The obstacles to be reconstructed are parameterized in table 1.

Example 1. D is a peanut-shaped, sound-soft obstacle. The measurement position is set to be on S_R with $R = 3$. This implies that the Hausdorff distance between D and S_R is less than two times the wavelength. Hence we indeed utilize the near-field rather than far-field measurements. Figure 1 presents the reconstruction results from the unpolluted data and polluted data with noise levels at 2% and 5%, respectively.

Example 2. We consider a sound-hard scatterer of a rounded-triangle shape. Near-field data are taken on $\{x: |x| = 5\}$. The Hausdorff distance between D and S_R is closed to four times the wavelength. See figure 2 for the reconstruction results.

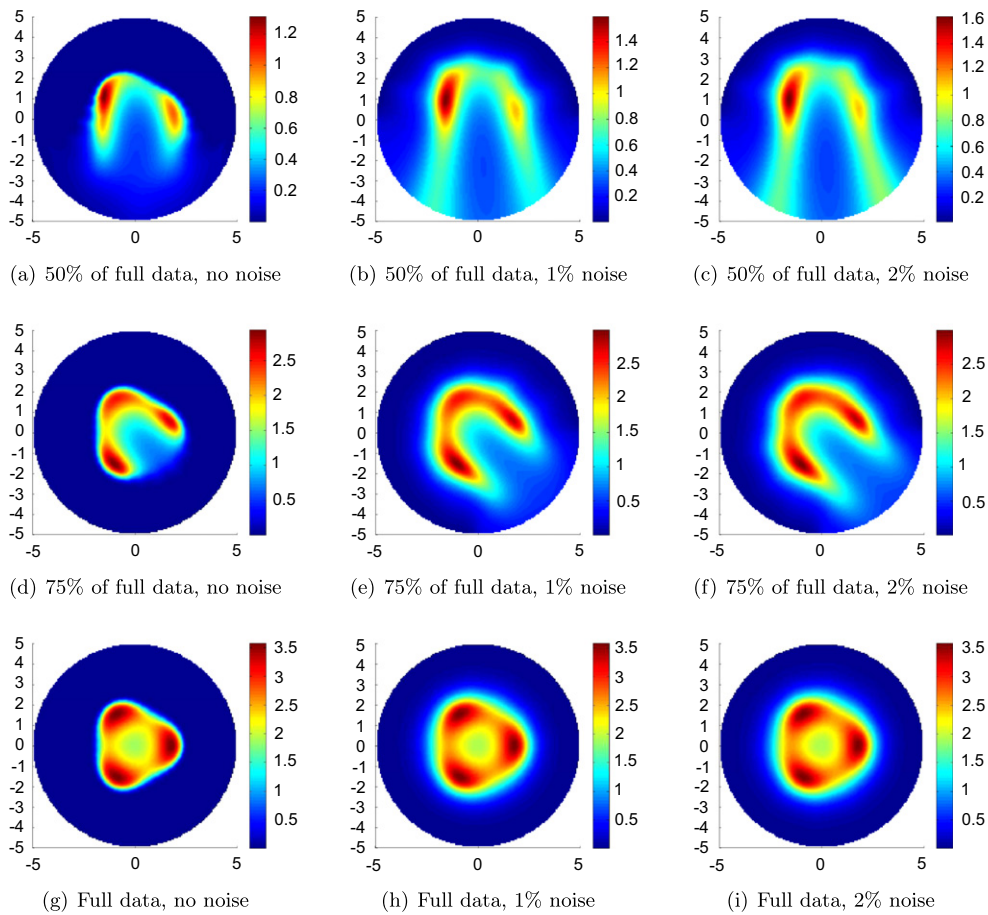


Figure 6. Reconstruction of a rounded triangle-shaped, sound-soft obstacle from limited and full near-field data at different noise levels. In (a)–(c), the obstacle is illuminated by point sources from the upper half-space. In (d)–(f), the point sources are uniformly distributed on $\{5(\cos \theta, \sin \theta) : \theta \in (0, 3\pi/2)\}$, while in (g)–(i) we have used point sources located on the full circle S_R with $R = 5$. The measurement positions of the scattered field coincide with the positions of the incident point sources.

Example 3. We consider the case when D is an apple-shaped obstacle with an impedance boundary condition. The impedance function is set to be $\rho(x(t)) = i(10 + 5 \sin t)$ with $t \in [0, 2\pi]$. Figure 3 presents the reconstruction results from the data without noise, with 2% noise and with 5% noise, respectively.

Example 4. D is a kite-shaped penetrable obstacle. The material inside D is supposed to be homogeneous with the constant wave number $k_1 = 9$. Figure 4 presents the reconstruction results from the data without noise, with 2% noise and with 5% noise, respectively.

Example 5. We consider the reconstruction of two sound-soft obstacles of different scales: a large-scale kite-shaped one, and a small-scale circle-shaped one with radius 0.2 and centered at $(1.4, -1.4)$. The wave number $k = 5$, so the wavelength is $\lambda \approx 1.257$. The distance between the two obstacles is approximately 0.8. The near-field is measured on $\{x : |x| = 5\}$. Figure 5 presents the reconstruction results from the data without noise, with 2% noise and with 5% noise, respectively.

Example 6. We compare the reconstruction results from the full near-field data and limited aperture near-field data at different noise levels. We set $k = 1$ and measure the near-field data on the sphere S_R with $R = 5$. This suggests that the Hausdorff distance between D and S_R is less than the wavelength $\lambda = 2\pi$. In figures 6(a–c), the incident acoustic point sources are uniformly distributed on the half-circle $\Gamma_R = \{R(\cos \theta, \sin \theta) : \theta \in (0, \pi)\}$ with the step size $\pi/64$, that is, the sound-soft obstacle is illuminated by 64 point source waves from above. In figures 6(d–f), 97 point source waves are generated from the three quarters of the circle S_R , that is, $\Gamma_R = \{R(\cos \theta, \sin \theta) : \theta \in (0, 3\pi/2)\} \subset S_R$. In figures 6(g–i), we used 128 incident point source waves uniformly distributed on the full circle S_R . In these tests, the near-field data are measured at the same positions as the incident point sources. The numerical reconstruction in figure 6 shows that using limited aperture near-field data provides only partial information of the scatterer. In particular, the un-illuminated part of the obstacle is not well-reconstructed.

From the above numerical experiments, it is seen that the factorization method with near-field data can provide good reconstruction results with a high resolution, especially in imaging impenetrable scatterers using the full near-field data. Moreover, we observe that the inversion scheme is indeed independent of the physical properties of the underlying obstacles.

Acknowledgments

The work of G Hu is financed by the German Research Foundation (DFG) grant HU 2111/1–2, and the work of B Zhang was partially supported by the NNSF of China grants 61379093 and 11131006. The authors thank the referees for their invaluable comments which helped improve the paper.

References

- [1] Arens T, Gintides D and Lechleiter A 2011 Direct and inverse medium scattering in a three-dimensional homogeneous planar waveguide *SIAM J. Appl. Math.* **71** 753–72
- [2] Colton D and Kress R 2013 *Inverse Acoustic and Electromagnetic Scattering Theory* 3rd edn (Berlin: Springer)
- [3] Hanke M and Kirsch A 2011 Sampling methods *Handbook of Mathematical Methods in Imaging* ed O Scherzer (Berlin: Springer) pp 501–50
- [4] Kirsch A 1998 Characterization of the shape of the scattering obstacle by the spectral data of the far field operator *Inverse Problems* **14** 1489–512
- [5] Kirsch A 2011 *An Introduction to Mathematical Theory of Inverse Problems* 2nd edn (Berlin: Springer)
- [6] Kirsch A and Kress R 1993 Uniqueness in inverse obstacle scattering *Inverse Problems* **9** 285–99
- [7] Kirsch A and Grinberg N 2008 *The Factorization Method for Inverse Problems* (Oxford: Oxford University Press)
- [8] Kirsch A 2007 An integral equation for Maxwell’s equations in a layered medium with an application to the factorization *J. Integral Equ. Appl.* **19** 333–58
- [9] McLean W 2000 *Strongly Elliptic Systems and Boundary Integral Equations* (Cambridge: Cambridge University Press)
- [10] Orispää M 2002 On point sources and near field measurements in inverse acoustic obstacle scattering *Doctorial Thesis* University of Oulu, Finland
- [11] Yang J, Zhang B and Zhang H 2013 The factorization method for reconstructing a penetrable obstacle with unknown buried objects *SIAM J. Appl. Math.* **73** 617–35
- [12] Yang J, Zhang B and Zhang H 2014 Reconstruction of complex obstacles with generalized impedance boundary conditions from far-field data *SIAM J. Appl. Math.* **74** 106–24